Electrochimica Acta 194 (2016) 26–39

Contents lists available at ScienceDirect

Electrochimica Acta

journal homepage: www.elsevier.com/locate/electacta

Conjugation of Azide-functionalised CdSe/ZnS Quantum Dots with Tetrakis(5-hexyn-oxy) Fe(II) phthalocyanine via Click Chemistry for Electrocatalysis

Siphesihle Robin Nxele, Tebello Nyokong*

Department of Chemistry, Rhodes University, Grahamstown 6140, South Africa

ARTICLE INFO

Article history:
Received 7 October 2015
Received in revised form 11 January 2016
Accepted 30 January 2016
Available online 18 February 2016

Keywords:
quantum dots
iron phthalocyanine
click chemistry
cyclic voltammetry
paraquat

ABSTRACT

In this work, azide-funtionalised CdSe/ZnS QDs are conjugated with tetrakis(5-hexyn-oxy) Fe(II) phthalocyanine for the electrocatalytic detection of paraquat. The conjugate was fully characterised using various techniques to confirm the success of the reaction. They also showed good electrocatalytic ability towards the electroreduction of paraquat with limits of detection (LoD) of 5.9×10^{-9} μM which is a great improvement compared to other reported sensors for this analyte.

© 2016 Elsevier Ltd. All rights reserved.

1. Introduction

Quantum dots (QDs) are semiconductor nanocrystals which have been widely studied for applications which include in *in vivo* imaging [1], molecular diagnostics of cancer [2] and biological detection [3]. However, not much research has gone into the electrocatalytic ability of QDs. It is only recently that QDs have been used alone or by combining them with other molecules for the electrocatalysis of various analytes [4–7]. Phthalocyanines (Pcs) on the other hand have been found to be good electrocatalysts [8], especially with electroactive central metals such as Co, Ni and Fe [9]. It has also been shown that combining QDs with phthalocyanines improves the electrocatalytic ability of the latter [10–12]. QDs have been linked to Pcs via an amide bond for electrocatalytic applications [10,11]. This work reports on the linking of QDs to alkynyl Fe phthalocyanine (represented as alkynyl FePc) via click chemistry. The QDs employed are the core shell azide modified CdSe/ZnS whose synthesis has been reported for click chemistry with transferrin, but in the current work 4-azidoaniline hydrochloride is employed rather than amino poly (ethylene glycol)-azide as the source of the azide group [13]. The current work is a first report of linking QDs to phthalocyanines by click chemistry. Click chemistry occurs by copper(I)-catalyzed azide-terminal alkyne cycloaddition (CuAAC) reaction [14]. This reaction provides functional-group selectivity and does not suffer the drawbacks of standard coupling reactions that are often susceptible to cross-linking. The ultimate goal is to develop a stable, sensitive and selective sensor for the detection of analytes using these semiconductor nanocrystals in combination with an alkynyl FePc. Paraquat is used as a test analyte.

Paraquat, formally known as 1,1-dimethyl-4,4-bipyridinium dichloride (Fig. 1) is a toxic pesticide that is highly resistant to biodegradation. For this reason, it is necessary to develop a highly stable and sensitive sensor for its detection. Numerous electrochemical sensors have been fabricated using different electrodes and modifiers for the determination of paraquat [15,16]. Paraquat has been electrochemically detected on Pc modified electrodes before [17], but is used in this work as a test analyte. We show in this work that very low detection limits are obtained when alkynyl FePc is clicked to QDs when compared to other Pc based electrodes.

2. Experimental

2.1. Reagents

1-Ethyl-3-(3-dimethylaminopropyl)-carbodiimide (EDC), N-hydroxyl succinimide (NHS) and 4-azidoaniline hydrochloride were purchased from Sigma–Aldrich. Tetrakis(5-hexyn-oxy)Fe(II) phthalocyanine (alkynyl FePc) was synthesized according to literature [18]. All other reagents were of analytical grade and

* Corresponding author. Tel.: +27 46 6038260; Fax: +27 46 6225109.
E-mail address: t.nyokong@ru.ac.za (T. Nyokong).

http://dx.doi.org/10.1016/j.electacta.2016.01.234
0013-4686/© 2016 Elsevier Ltd. All rights reserved.

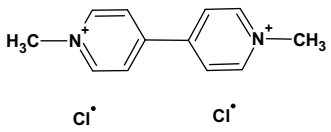


Fig. 1. Structure of paraquat.

used as received. Glutathione (GSH) capped CdSe/ZnS QDs (represented as GSH QDs) were synthesized as reported before [19].

2.2. Synthesis

2.2.1. Functionalization of the CdSe/ZnS QDs with azide

The conjugation reaction carried out was adapted from a method in literature [20]. The covalent linkage was carried out as follows: GSH QDs (40 mg) were dissolved in 2 mL of water. Thereafter EDC (0.019 g, 0.1 mmol) and NHS (0.012 g, 0.1 mmol) were introduced into the solution in order to activate the carboxyl functional moiety of the GSH capping the QDs. The reaction was left stirring at room temperature for 2 h after which 2 mL solution of 20 mg (0.117 mmol) of 4-azidoaniline hydrochloride were added. The solution was left stirring for 24 h thereby leading to the formation of the carbonamide linkage between the GSH QDs and 4-azidoaniline hydrochloride. The QDs were precipitated out of solution with ethanol and were successively purified with methanol. The QDs are represented as azide QDs (Scheme 1).

2.2.2. Functionalization of azide QDs with FePc (Clicked FePc-QDs)

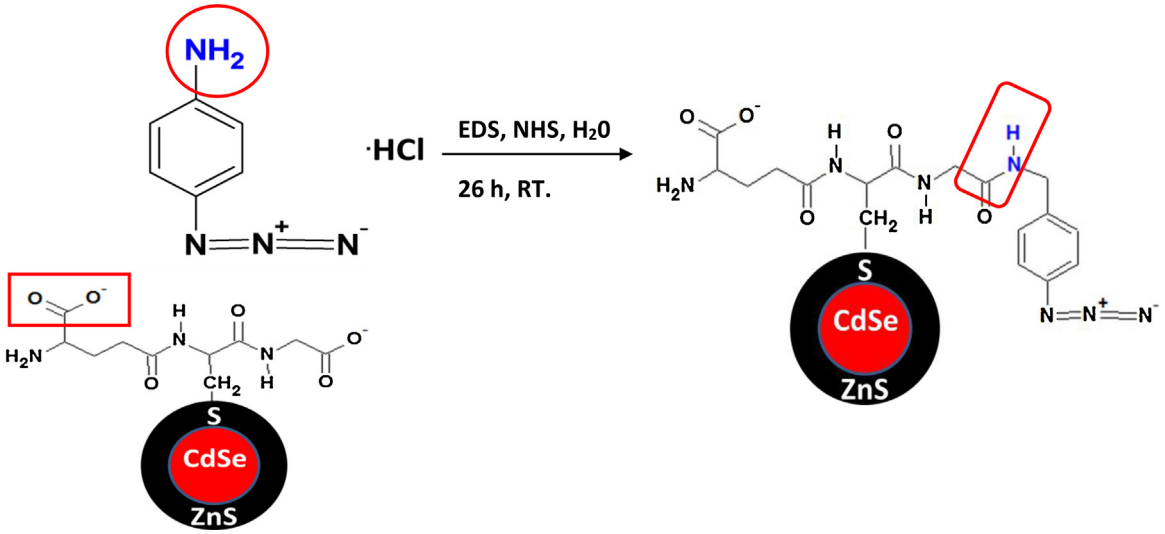
Alkynyl FePc (9.50 mg, 1.00 mmol), azide QDs (130.0 mg), $CuSO_4.5H_2O$ (12.5 mg, 5.00 mmol,) and sodium ascorbate (79.0 mg, 40.0 mmol) were dissolved in 10 mL of dimethylformamide (DMF). The mixture was stirred at room temperature for 48 h under Ar. The reaction mixture was then poured into 100 mL of cold water. The precipitate was filtered off and washed with water, until the filtrate was neutral. The crude residue was crystallized from methanol to give the desired product which was the clicked FePc-QDs. Yi IR (KBr) ν_{max}/cm^{-1}: 1464, 1621 (triazole N_3); 3201 (C=CH); 2167 (C=C), 2926(NH_2); 1607 (carbonamide) (Scheme 2).

2.3. Equipment

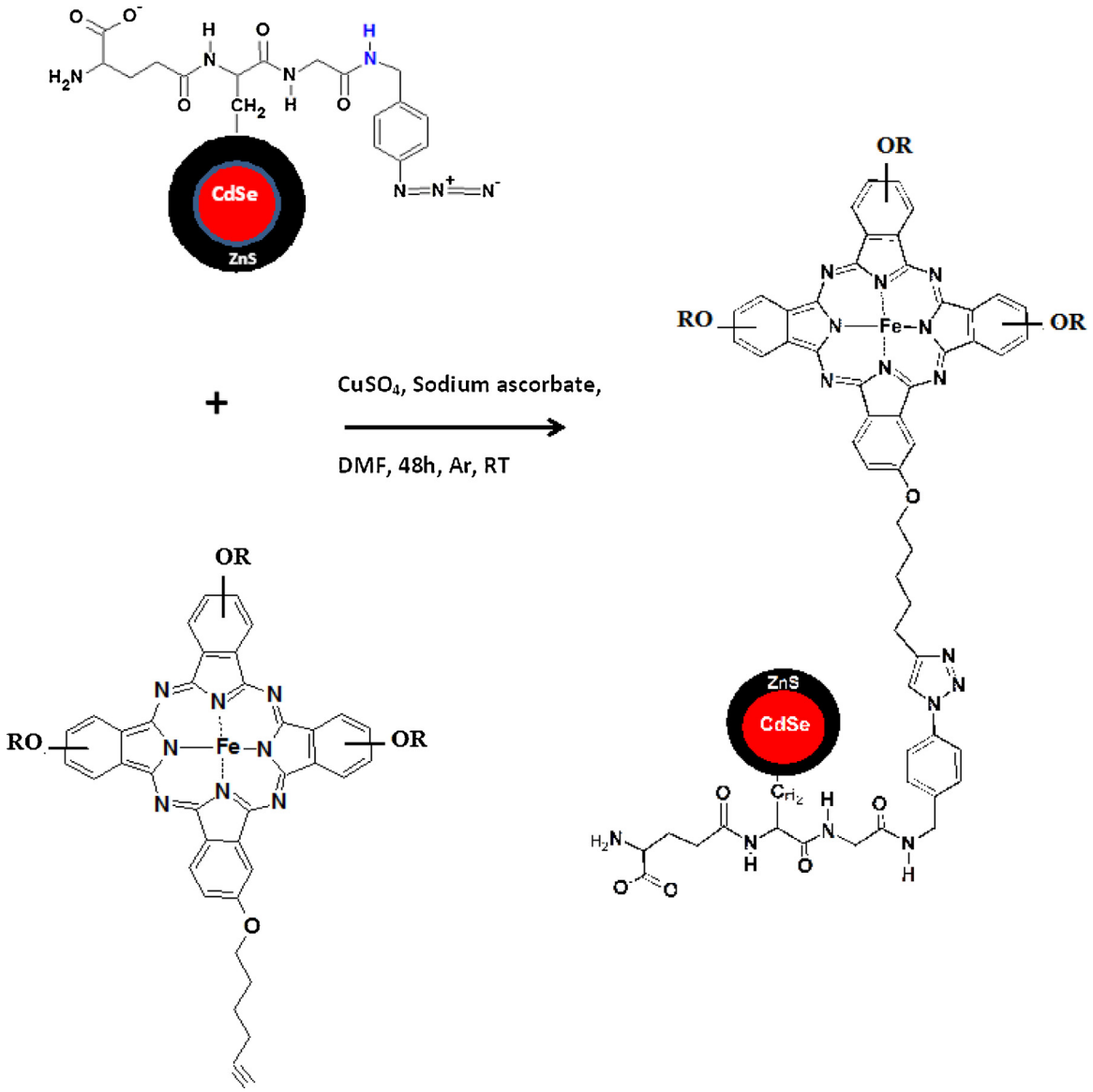
Ground state electronic absorption spectrum was obtained at room temperature using a Shimadzu UV-2550 spectrophotometer. Fluorescence emission spectra were recorded on a Varian Eclipse fluorescence spectrofluorimeter. Infra-red spectra were collected on a Bruker Alpha model FT-IR Spectrometer with platinum ATR. Transmission electron microscope (TEM) micrographs of the QDs were obtained using a Zeiss Libra 120 TEM operating at 80 kV. X-ray powder diffraction patterns were recorded on a Bruker D8 Discover equipped with a LynxEye detector, using Cu Ka radiation (l = 1.5405 A°, nickel filter). Data were collected in the range from $2\theta = 5°–60°$, scanning at $1°\ min^{-1}$ with a filter time-constant of 2.5 s per step and a slit width of 6.0 mm. Samples were placed on a zero background silicon wafer slide. The X-ray diffraction data were treated using EVA (evaluation curve fitting) software. Baseline correction was performed on each diffraction pattern.

Scanning electrochemical microscopy (SECM) experiments were conducted using Uniscan equipment, model 370 and a 15 μm Pt microelectrode as the tip. Pt counter and Ag/AgCl wire pseudo-reference electrodes were employed. Approach curve analysis and constant height imaging were employed. For surface imaging, the microelectrode tip was maintained at a constant height (Z) and the desired area scanned along the the X-Y plane. Changes were monitored in the steady state current of $K_3[Fe(CN)_6]$ oxidation at 0.1 V vs. Ag|AgCl as the tip travels.

X-ray photoelectron spectroscopy (XPS) was done using a Kratos Axis Ultra DLD, with the Al (monochromatic) anode, equipped with a charge neutraliser. For wide XPS scans, the following parameters were used: emission 10 mA, anode (HT): 15 kV, operating pressure below 5×10^{-9} Torr, hybrid lens, and resolution to acquire scans was at 160 eV pass energy in slot mode. The centre used for the scans was at 520 eV and the width at 1205 eV, with steps at 1 eV and dwell time at 100 ms. For the high resolution scans, the resolution was changed to 40 eV pass energy



Scheme 1. Conjugation reaction between GSH QDs and 4-azidoaniline hydrochloride to form azide QDs.



Scheme 2. Click chemistry between alkynyl FePc and azide QDs.

in slot mode. Centre was at 402 eV and width at 12 eV for N(1s), with step size at 0.05 eV and dwell time at 500 ms.

Glassy carbon plate electrodes (1 cm × 1 cm and 2 mm thick) obtained from Goodfellow, UK were used for the SECM and XPS analyses.

Cyclic and differential pulse voltammetry experiments were run using the Autolab PGStat electrochemical workstation. A three-electrode system, with a pseudo Ag|AgCl reference electrode, a Pt counter electrode and a glassy carbon electrode (GCE) as the working electrode was employed. The GCE was cleaned by polishing on a Beuhler 1200 grit Microcut® Disc using 3 μm and then 0.25 μm diamond paste (MetaDi® supreme polycrystalline diamond suspension, Beuhler) followed by polishing on a Beuhler felt pad using aluminium oxide powder before use. The GCE was thoroughly rinsed with Milli-Q water before each experiment. The electrode was modified by drop dry method whereby a drop 1 μL alkynyl FePc, clicked FePc-QDs, azide QDs or GSH QDs in DMF was placed on the electrode followed by drying.

3. Results and Discussion

3.1. Characterisation of CdSe/ZnS QDs and their conjugates

Scheme 2 shows the route for the click reaction between alkynyl FePc and azide CdSe/ZnS QDs. The size of the Pcs is approximately of 1 nm while the size of the quantum dots is ~6 nm (as determined by XRD below). Hence, it is likely that more than one Pc can be bonded to the QDs considering the size of Pc relative to QDs. The reverse where more than one QD bind to a Pc is unlikely due to size considerations. The number of Pcs bonded to the QDs was estimated to be 60:1 (Pc:QDs) following literature methods, but using absorption instead of fluorescence [21]. This number is

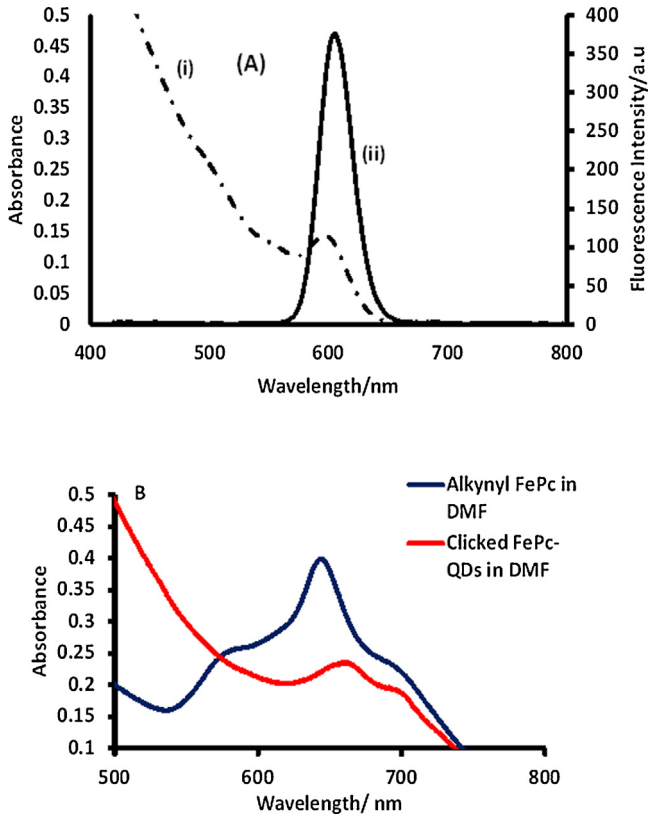


Fig. 2. **(A)** UV/vis absorption (i) and emission (ii) spectra of GSH QDs in chloroform. **(B)** UV/vis spectra of alkynyl FePc alone and clicked FePc-QDs both in DMF.

similar to that obtained (70 Pc per QD) for electrostatic binding of other Pcs to QDs [21].

3.1.1. UV/vis and Emission Spectra

Fig. 2**A** illustrates the **(i)** absorption and **(ii)** emission spectra of the synthesised QDs which absorb at 596 nm and emit at 605 nm. The spectra show the typical broad absorption and narrow emission spectra. We have recently reported the UV–vis spectra (Fig. 2**B**) of alkynyl FePc [18] which showed the presence of μ-oxo species (near 590 nm), with some monomeric species (near 630 nm) and a shoulder near 700 nm. On linking alkynyl FePc to QDs via click chemistry, there is a clear split in the Q band, Fig. 2**B**. A split Q band and a shifting of one of the Q band components to longer wavelengths is typical of the oxidation of Fe(II) Pc to Fe(III) Pc derivatives [22]. Fig. 2**B** suggests the presence of both Fe(II) Pc and Fe(III) Pc species.

3.1.2. Transmission Electron Microscopy (TEM)

Fig. 3**(i)–(ii)** shows the TEM images and size distribution of the GSH QDs and the azide QDs respectively. It is evident that some aggregation has occurred in **(i)** but there some degree of monodispersity. The average size was found to be 5.59 nm with a standard deviation of 1.78 nm, Fig. 3**(i)**. The histogram beside Fig. 3**(i)** shows that the majority of these nanocrystals fall in the size range 4–7 nm. Once functionalized with azide groups, the particle distribution as well as particle size slightly increases as shown by Fig. 3**(ii)** and the corresponding histogram. Fig. 3**(iii)** shows an image of the clicked FePc-QDs which shows a high degree of aggregation making it difficult to estimate the particle size after conjugation. Phthalocyanines in general are known to aggregate [22].

3.1.3. X-ray Diffraction

XRD was also used to characterise the QD in order to confirm their formation and to determine the size according to the Scherrer equation. The diffractogram obtained is shown in Fig. 4. The three characteristic peaks of the QDs were observed and confirmed by literature [20]. The sizes of the QDs were also estimated by using the Scherrer equation Eq. (1) [23]:

$$d(\text{Å}) = \frac{k\lambda}{\beta cos\theta} \quad (1)$$

where λ is the wavelength of the X-ray source (1.5405 Å), k is an empirical constant equal to 0.9, β is the full width at half maximum of the diffraction peak and θ is the angular position. The size of the GSH QDs was determined to be 5.8 nm which does not vary too much with the average size determined from TEM.

3.1.4. Infrared Spectroscopy

Fig. 5 shows the FTIR spectra of the GSH QDs, 4-azidoaniline hydrochloride, azide QDs, alkynyl FePc and clicked FePc-QDs. The GSH QDs spectrum shows the characteristic amine stretch and carbonamide stretch at 2926 cm^{-1} and 1607 cm^{-1}, respectively. For the azide QDs, a small stretch at 2142 cm^{-1} may be attributed to the azide group and it is also observed in the spectrum of 4-azidoaniline hydrochloride. The NH_2 stretch observed at 2926 cm^{-1} in GSH QDs has almost disappeared in azide QDs and the amide linkage has decreased in intensity. Once the azide QDs

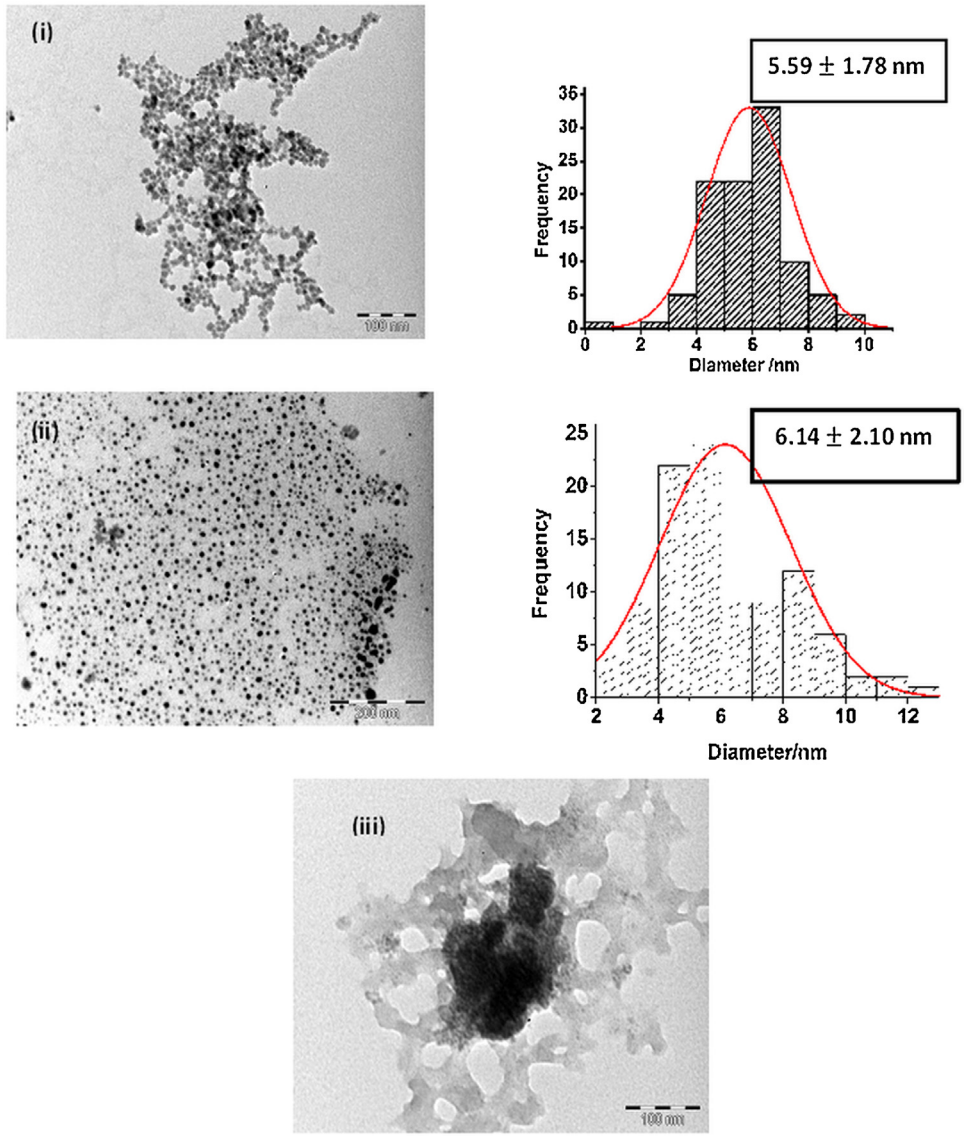


Fig. 3. TEM images of **(i)** GSH QDs in water (with corresponding histogram), **(ii)** Azide QDs in DMF (with corresponding histogram) and **(iii)** clicked FePc-QDs in DMF.

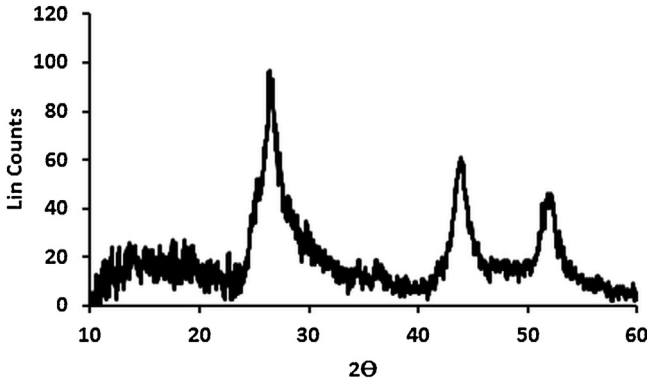


Fig. 4. XRD patterns of GSH QDs.

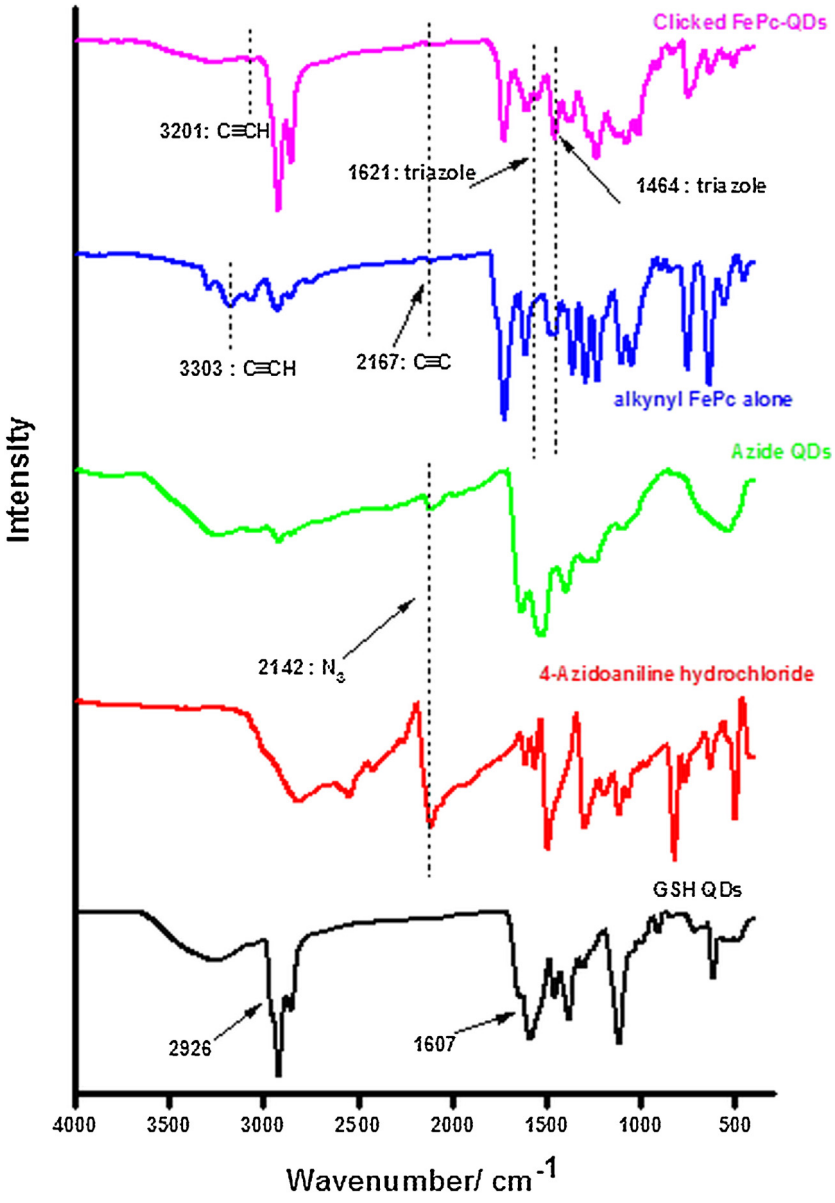


Fig. 5. FTIR spectra of the GSH QDs, 4-azidoaniline hydrochloride, azide QDs, alkynyl FePc and clicked FePc-QDs.

have been clicked with the FePc the azide peak seems to have almost disappeared, however, the NH_2 peak due to the GSH capping of the QDs appears to be intense again which may be a result of the NH_2 being more exposed. Weak stretches due to the terminal alkyne groups of the FePc are still observed which implies that not all groups were involved in bonding. These observed changes indicate successful conjugation. However, XPS will be used below to confirm this conclusion.

3.1.5. X-ray Photoelectron Spectroscopy (XPS)

XPS was used to confirm the presence of the functional groups of interest on the molecules studied as well as the success or failure of the surface modification process of the electrode. The bare glassy carbon plate (GCP) shows the expected carbon peak as well as with an oxygen peak, the latter due to adsorbed oxygen, Fig. 6. These peaks are also observed on the other plates but with differing intensities due to the nature of the surface. The Fe(2p) peaks are not intense but are observed for clicked FePc-QDs, Fig. 6.

The N(1s) peak is due to the nitrogens of the GSH capping of the GHS-QDs. The presence of these peaks confirms the presence of the GSH-capped QDs on the surface of the GCP. After functionalising the QDs with azide groups, the same peaks due to the QDs are observed but the peak intensities are lower which suggests a change in the surface chemistry of the plate.

Fig. 7**A** shows the high resolution scan of the N1s region of the GSH QDs. The main peak appears at a binding energy of 400 eV and seems to split into two. By deconvoluting this peak, three peaks are observed at binding energies of 399.1 eV, 399.7 eV and 400.8 eV. The peak at the lowest binding energy is due to the N-H of the GSH capping of the GHS QDs. The peak at 400.8 eV may be attributed to the C-N of the GSH capping [24]. The peak observed at 399.7 eV may be a combination of the C-N and N-H signals.

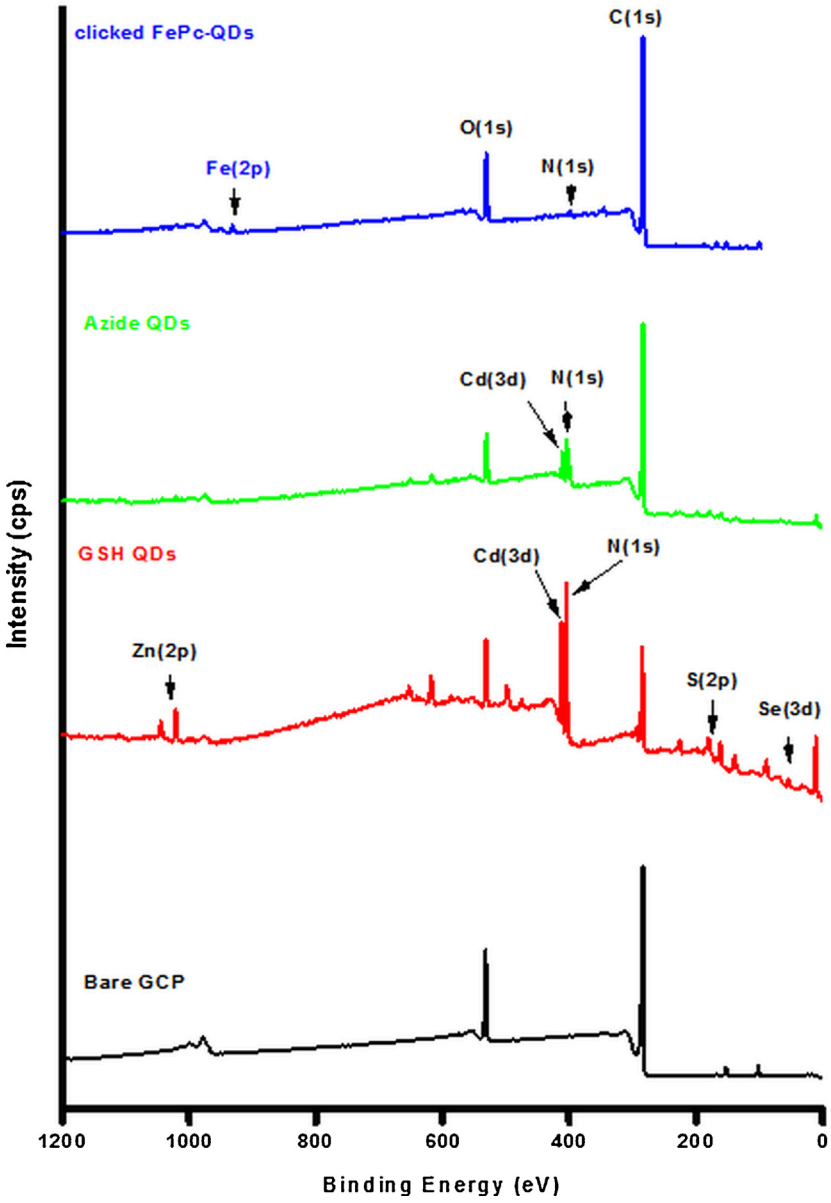


Fig. 6. XPS wide scans of bare GCP, GSH QDs, azide QDs and clicked FePc-QDs on a GCP.

Fig. 7**B** shows the high resolution spectrum of the azide-functionalised QDs as well as the spectrum for the clicked FePc-QDs. The peak due to the electron deficient central nitrogen is observed at a binding energy of 404.6 eV. The peak at 399.6 eV is due the two outer nitrogens of the azide group (neutral and negatively charged nitrogens) [25–28]. It is possible that if there is GSH-capping still exposed it may contribute to the nitrogen signal as well but the binding energies observed suggest the presence and dominance of the azide groups on the surface. The ratio of these peaks is expected to be 2:1 [26] but deviations have been observed in some studies [25,28,29] and said to be a result of degradation after a certain period of analysis under the destructive XPS conditions [30]. Upon clicking the QDs with the FePc, the intensities of these peaks decreases and there is a chemical shift observed. The peaks are observed at binding energies of 399.4 eV and 405.5 eV.

3.1.6. Scanning electrochemical microscopy (SECM)

Fig. 8**(A)** shows the approach curves resulting from the different electrode surfaces tested in a ferricyanide solution. GSH QDs and azide QDs proved to be insulating as expected. The bare GCP and the ones modified with the FePc alone and clicked FePc-QDs proved to be conducting. Alkynyl FePc alone or when mixed with azide QD was less conducting compared to clicked FePc-QDs, showing the importance of clicking.

3.2. Characterization of modified electrodes by Cyclic (CV) and Differential pulse (DPV) voltammetry

Fig. 9 shows the CVs of GCE electrode modified with the GSH QDs, azide QDs, alkynyl FePc, QDs mixed with FePc (not conjugated) and the clicked FePc-QDs in a ferricyanide solution. The electrodes that were less conducting (larger cathodic to anodic

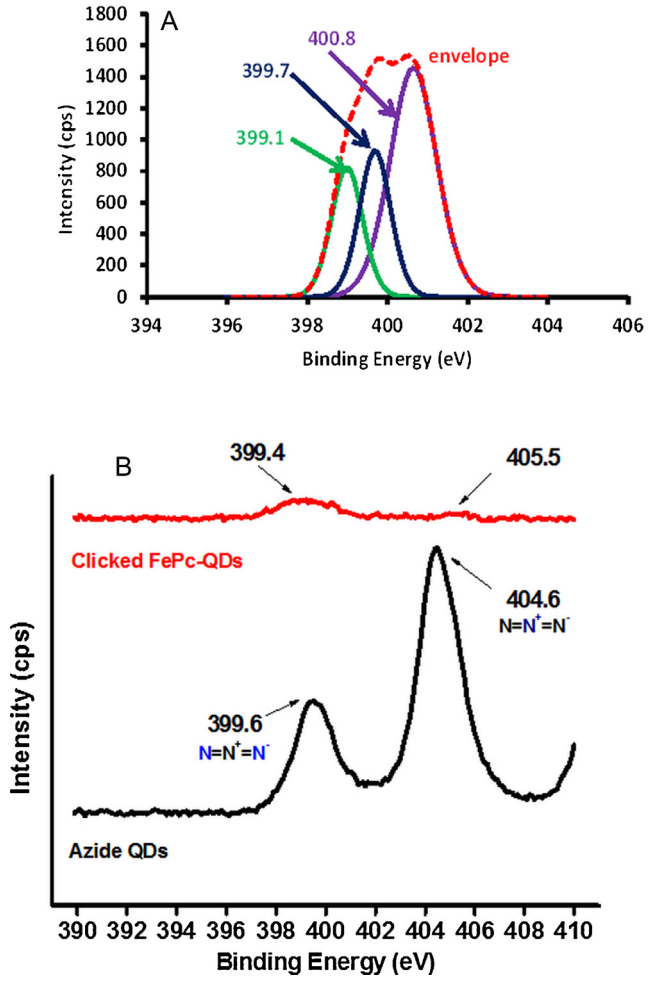


Fig. 7. High resolution scans of **(A)** GSH QDs (deconvoluted), **(B)** azide- QDs and clicked FePc-QDs.

peak separation, ΔE) were the ones modified with GSH QDs and azide QDs. For the mixture of QDs and alkynyl FePc, there were no clear peaks, Table 1. Of all the modified electrodes, alkynyl FePc alone was the most conducting followed by clicked FePc-QDs in the ferricyanide solution, Table 1.

The modified electrodes were also tested in a 0.1 M NaOH solution. The reason for this is that the analyte of interest is dissolved and studied in this solution. The peaks due to alkynyl FePc were identified using DPV (Fig. 10), since the CV scans were not clearly defined.

Fig. 10**A** shows two peaks for adsorbed alkynyl FePc. The more prominent peak is observed at −0.57 V with a peak current of 2.5 μA and the other peak is observed at 0.34 V with a peak current at 1.4 μA for alkynyl FePc alone, Fig. 10A. The peak at lower potentials may be attributed to the Fe(II)/Fe(I) redox pair and the peak at more positive potentials may be attributed to the Fe(III)/Fe (II) redox pair [9,31,32]. It is expected that the Fe(II)/Fe(I) redox pair will catalyse the reduction of the analyte of interest (paraquat).

In order to assign peaks when the FePc and QDs are combined, DPV was used to analyse the redox processes of the QDs alone (Fig. 10**B**). Three peaks were observed at −1.07 V, −0.52 V and −0.29 V. The peaks at −1.07 V and −0.5 V may be attributed to the reduction of the ZnS shell and the CdSe core, respectively [33]. The peak at −0.29 V has been associated with the reduction of Cd and therefore may be associated with the reduction of the CdSe core [34].

Fig. 10**(C)** shows the DPV of the clicked FePc-QDs in a 0.1 M NaOH solution. The shapes of the peaks are similar to those for alkynyl FePc alone in Fig. 10**(A)**, and are most likely overlapping with the DPV peaks of QDs. The peak near −0.5 V may be due to the Fe(II)/Fe(I) redox pair in comparison with alkynyl FePc alone. This process will be involved in the electrocatalytic reduction of paraquat.

3.3. Electrocatalytic detection of paraquat

3.3.1. SECM studies

Fig. 8**(B)** shows the approach curves of GCP modified with alkynyl FePc alone, QDs mixed with alkynyl FePc and clicked FePc-QDs in 2 mM paraquat. Alkynyl FePc alone shows larger currents as the microelectrode was approaching the surface but much closer to the surface we see the clicked FePc-QDs showing higher maximum current.

Area scans are generally used to determine how the surface topography changes due to the interaction of the solution with the electrocatalyst on the surface of the electrode. Fig. 8**C(i)-(iii)** show

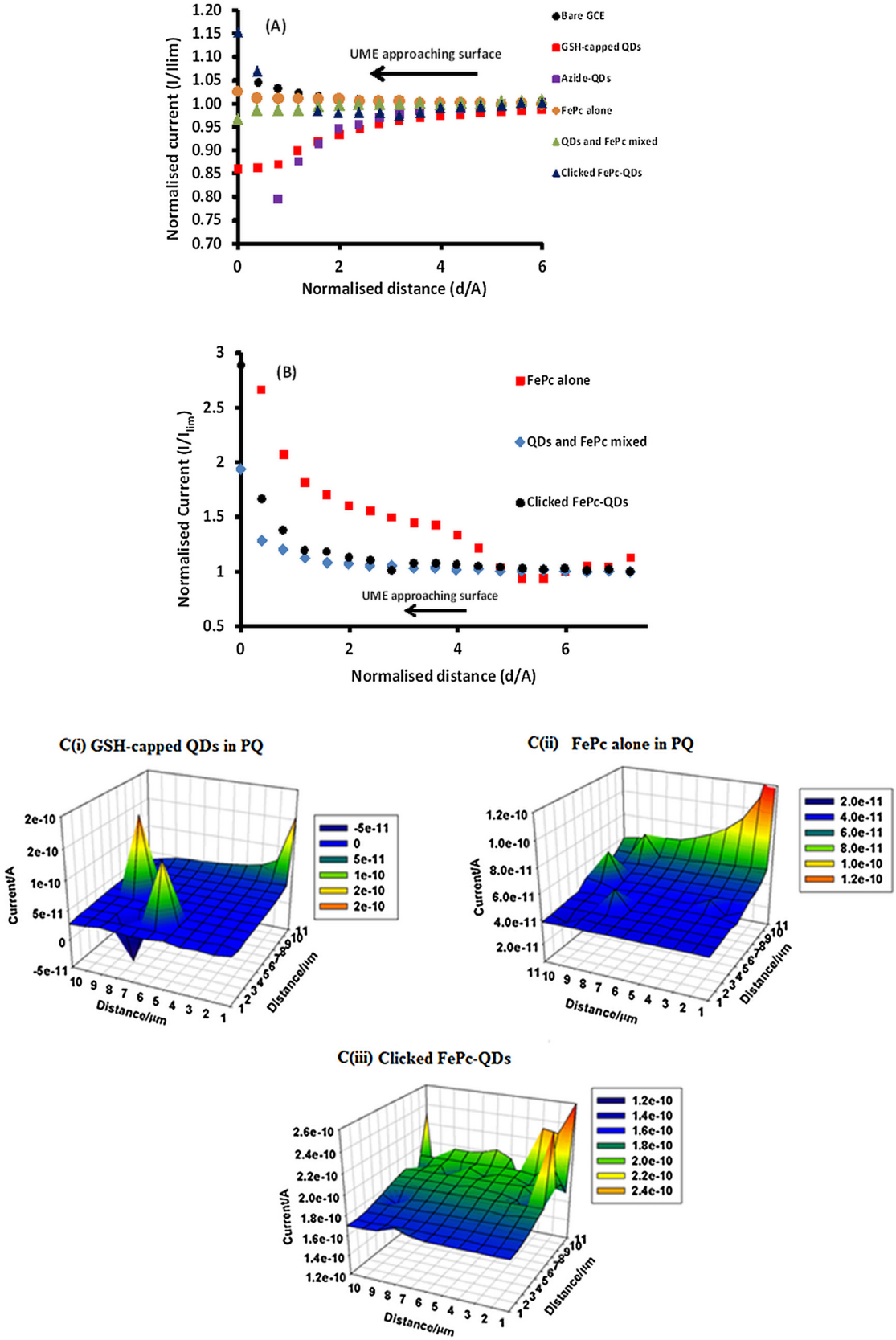


Fig. 8. Approach curves of GCP with different surface modifications in **(A)** 2 mM $K_4[FeCN_6]$ and **(B)** 2 mM paraquat. **(C)** Area scans of **(i)** GSH-capped QDs, **(ii)** FePc alone and **(iii)** clicked FePc-QDs in 2 mM paraquat solution (in 0.1 M NaOH).

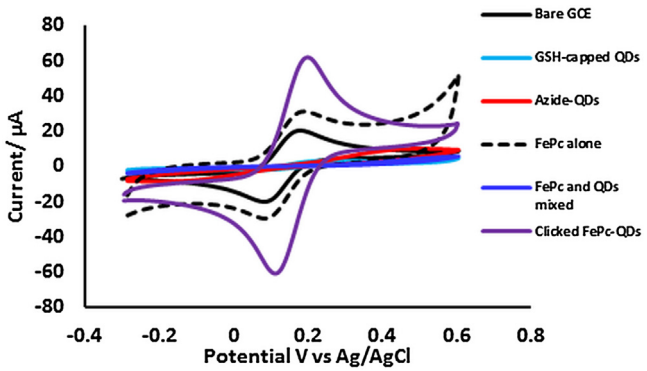


Fig. 9. Modified electrodes in a 2 mM ferricyanide solution with KCl as the supporting electrolyte. Scan Rate: 50 mV/s.

area scans of the QDs alone, alkynyl FePc alone and clicked FePc-QDs in a paraquat solution. The clicked FePc-QDs also show higher currents than the other two surfaces tested. This gives some confidence with regards to the potential of the sensor constructed in the work reported.

3.3.2. Cyclic voltammetry

The CVs for modified electrodes in paraquat are shown in Fig. 11. Two redox processes were observed (labelled **P1** and **P2**) on the bare electrode and on the Pc based electrodes. When the azide QDs and alkynyl FePc are just mixed with no conjugation reaction to achieve any formal bonding, the current response is weaker than for clicked FePc-QDs, confirming the advantage of using click chemistry for the development of electrocatalysts for the detection of paraquat (PQ). It can also be concluded that the Fe(II)/Fe(I) redox pair (Fig. 10**C**) catalyses the electroreduction of paraquat since it is observed in the same potential region as the paraquat peaks are observed (Fig. 11).

The reason for there being two peaks is said to be a result of the reduction of the positively charged nitrogens present in the molecule. The proposed mechanism is shown by Eqns. (2),(3) [35]:

$$\text{Paraquat}^{2+} + e^- \rightarrow \text{Paraquat}^{+} \quad (2)$$

$$\text{Paraquat}^{+} + e^- \rightarrow \text{Paraquat}^{\circ} \quad (3)$$

The first equation is attributed to the peak denoted as P2 and the second equation is attributed to the peak denoted P1 (Fig. 11) [35].

Table 1
Potential difference of modified electrodes tested in 2 mM $K_4[FeCN_6]$.

Electrode	ΔE/mV (vs Ag|AgCl)
Bare	86
GSH-QDs	172
Azide-QDs	303
FePc alone	71
QDs-FePc mix	[a]
clicked FePc-QDs	85

[a] no peaks observed.

Since it has been established that the Fe(II)/Fe(I) redox pair of the phthalocyanine catalyses the reduction of paraquat, the mechanism may be illustrated by Eqns. (4)–(6):

$$[Fe^{II}Pc] + e^- \rightarrow [Fe^{I}Pc]^- \quad (4)$$

$$\text{Paraquat}^{2+} + [Fe^{I}Pc]^- \rightarrow [PQ - Fe^{I}Pc]^+ \quad (5)$$

$$[PQ - Fe^{I}Pc]^+ \rightarrow Fe^{II}Pc + PQ^+ \quad (6)$$

where Fe(II) in Fe(II) Pc is initially reduced (4), followed by the adsorption of paraquat **(5)** (confirmed before [17]) and its subsequent reduction (6). PQ^+ would be reduced further in the same manner.

3.3.3. Determination of detection limits

The electrodes modified with alkynyl FePc alone and clicked FePc-QDs were used to for the determination of detection limits. The results obtained are illustrated by Fig. 12**A** and Fig. 12**B** where the concentrations analysed ranged between 0.8 and 1.33 μM. The insets show a linear relationship between the concentration and the peak currents for both P1 and P2. The limit of detection for both electrodes was determined using the 3δ-notation where δ is the standard deviation and 3 is a recommended factor that gives a practical confidence of 90% to 99.7% [36–38]. The limit of detection (see Table 2) for the alkynyl FePc alone (using P2) was found to be of the same order of magnitude as some of the Pc based electrodes reported in literature in literature for the detection of paraquat [17,39]. However, upon testing clicked FePc-QDs, the limit of detection improved compared to alkynyl Pc alone which proves the quality and good potential of the work. The paraguat detection was the lowest for clicked FePc-QDs when compared to literature reports for Pc based electrodes [17,38],Table 2. The Interim Maximum Acceptable Concentration (IMAC) for PQ as a dichloride in drinking water has been reported as 10 μg/L (3.88×10^{-8} M) [40], which is higher than the value for clicked FePc-QDs determined in this work.

3.3.4. Electrode Kinetics

By changing the scan rate, the chemical processes that occur during the electrocatalysis of paraquat can be determined. Fig. 13**A** shows the CVs of the clicked FePc-QDs in paraquat at different scan rates. Fig. 13**B** shows the plot of current vs scan rate where an initial linear increase in current with scan rate is observed until a limit is

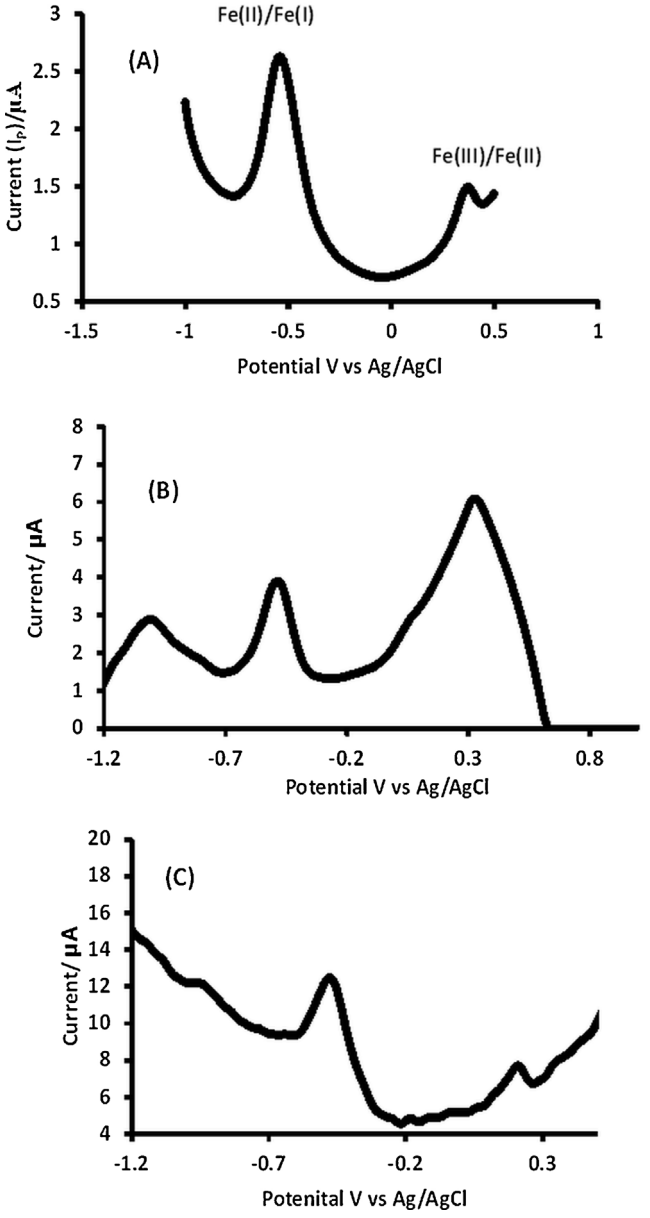


Fig. 10. DPV of **(A)** alkynyl FePc, **(B)** GSH QDs and **(C)** clicked FePc-QDs in 0.1 M NaOH.

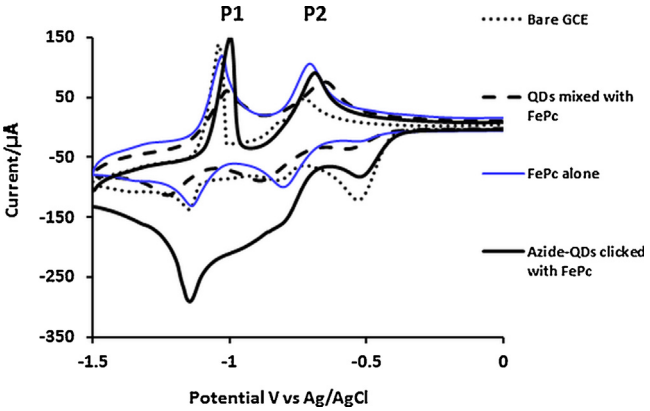


Fig. 11. Cyclic voltammogram of bare and modified electrodes in 2 mM paraquat solution (in 0.1 M NaOH). Scan rate: 50 mV/s.

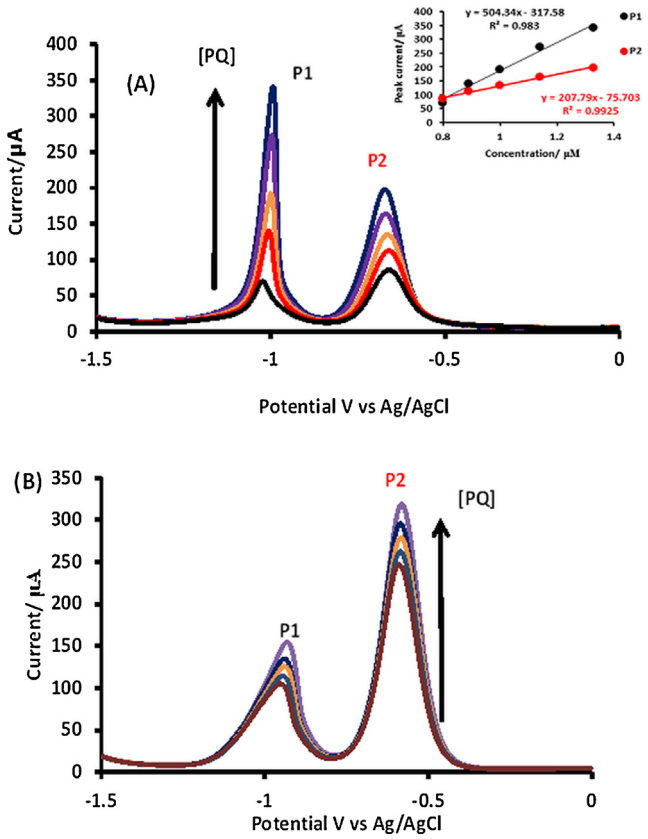


Fig. 12. (A) DPV of alkynyl FePc adsorbed on electrode in 0.1 M NaOH with increasing paraquat concentration and (**B**) DPV of clicked FePc-QDs in 0.1 M NaOH with increasing paraquat concentration. Concentration range = 0.8 μM to 1.33 μM. Insets: Plots of concentration vs peak current for P1 and P2.

reached and almost levels off from 200 mV/s. This may be a result of slow electron transfer from the electrode surface which would then limit the redox reactions at these high scan rates between the paraquat species and the electrocatalyst [41]. This behavior has been observed in literature for paraquat detection where an initial diffusion process is observed at lower scan rates followed by the observation of an adsorption process at higher scan rates [42]. It has also been reported that deviations from linearity as observed In Fig. 13**B** is more likely a result of a limit in surface kinetics rather than resistance in solution [43]. Fig. 13**C** however, shows the plot of peak current vs the square root of the scan rate which yielded a linear plot. This relationship indicates that the process is diffusion controlled [14] at low scan rates, rather than being an adsorption process as observed in previous studies involving paraquat [17]. These observations imply that at high scan rates, there is a degree of passivation of the electrode surface resulting in the deviations from the relationship between current and scan rate that is initially observed.

Table 2
Summary of LoD results obtained in comparison with other paraquat electrochemical sensors reported in literature.

Electrode[a]	LoD/M	Technique	Reference
rGNS-2/MWCNT/CoTAPc/GCE	3.32×10^{-8}	SWV	[17]
Pc/PGE	$\sim 1 \times 10^{-6}$	SWV	[38]
FePc/GCE	1.3×10^{-8}	DPV	This work
FePc-CdSe/ZnS QDs-GCE	5.9×10^{-9}	DPV	This work

[a] MWCNT = multiwalled carbon nanotubes, TAPc = tetraamino phthalocyanine, PGE = pyrolitic graphite electrode.

3.4. Interferences

Paraquat may occur in the presence of other agrochemicals which may, in turn interfere with the signal upon the detection of this analyte. It is thus of paramount importance that it be established how and to what extent these interferences may occur. No formal experiments on real samples or in the presence of interferences have been conducted in this work but there are a number of reports that have shown the effects that certain chemical species may have with respect to paraquat detection. Examples of interferences that could occur in real samples include metal ions such as Cd(II), Cu(II), Pb(II) and Zn (II) where the constructed sensors were resistant to fouling to up to 10-fold excess of the interfering ions with no significant change in the peak current produced [15,44]. These metal ions are said to interfere with the detection of paraquat due their competing for complexation with the electrocatalyst or modifier [45]. A study however, showed that ethylenediaminetetraacetic acid (EDTA) minimized interferences from these common metal ions [46] and another showed that addition of KCN to the analytical solution minimized the interferences [45]. Other agrochemicals that have been studied in the presence of paraquat include diuron, amitrole, atrazine and urea using the mixed solution method [12]. It was determined that diuron had minimal interference upon paraquat detection. The other chemicals on the other had proved to interfere strongly leading to the conclusion that pre-treatment would be required in order to obtain reliable results when testing for paraquat in their presence.

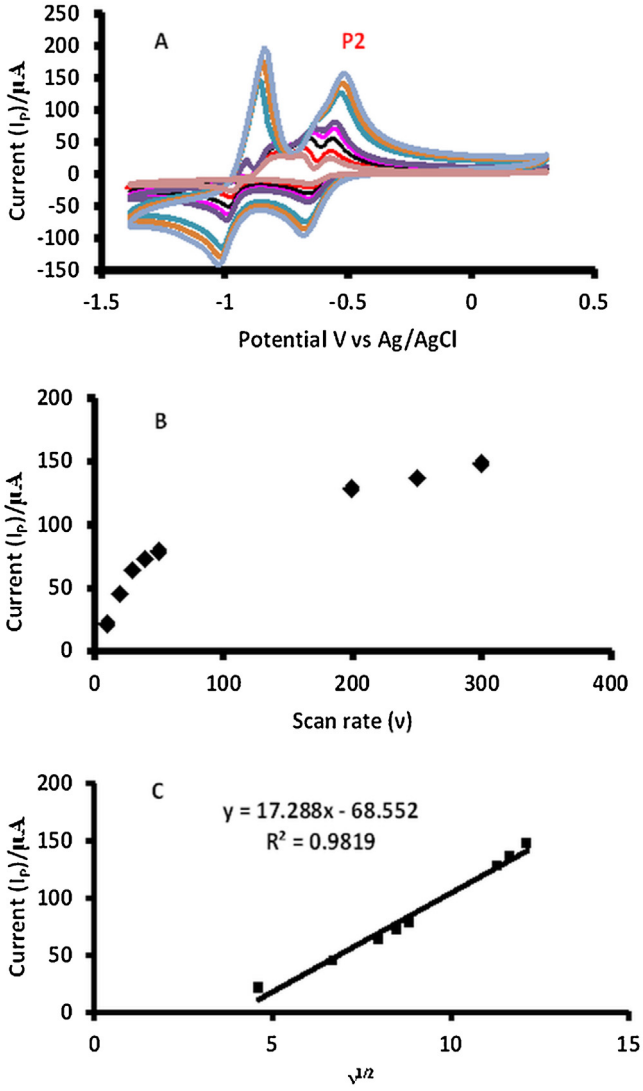


Fig. 13. (A) Cyclic voltammograms of clicked FePc-QDs in 2 mM paraquat solution obtained with scan rates of 10, 20, 40, 60, 80, 100, 150, 200, 250 and 300 mV/s. **(B)** Plot of I_P vs scan rate (ν) and **(C)** Plot of I_P vs the square root of the scan rate ($\boldsymbol{\nu^{1/2}}$).

4. Conclusion

Azide functionalized CdSe/ZnS QDs were successfully and clicked to alkynyl FePc giving clicked FePc-QDs. The latter was characterized using many techniques including XPS. The electrocatalytic behaviour of the clicked FePc-QDs towards paraquat was also studied using various voltammetry techniques and scanning electrochemical microscopy. The limit of detection (LoD) determined in this work was lower than some reported values as well as internationally allowed limits proving that the sensor constructed in this work is efficient for the electrocatalysis and analysis of paraquat.

Acknowledgements

This work was supported by the Department of Science and Technology (DST) and National Research Foundation (NRF), South Africa through DST/NRF South African Research Chairs Initiative for Professor of Medicinal Chemistry and Nanotechnology (UID = 62620) as well as Rhodes University and DST/Mintek Nanotechnology Innovation Centre (NIC) – Sensors, South Africa.

References

[1] B. Dubertret, P. Skourides, D.J. Norris, V. Noireaux, A.H. Brivanlou, A. Libchaber, In Vivo Imaging of Quantum Dots Encapsulated in Phospholipid Micelles, Science 298 (2002) 1759–1762.
[2] P. Juzenas, W. Chen, Y.-P. Sun, M.A. Coelho, R. Generalov, N. Generalova, I. Christensen, Quantum Dots and Nanoparticles for Photodynamic and Radiation Therapies for Cancer, Adv. Drug Deliv. Rev. 60 (2008) 1600–1614.
[3] S.P. Wang, N. Mamedova, N.A. Kotov, W. Chen, Antigen/Antibody Immunocomplex from CdTe Nanoparticle Biconjugates J.Studer, Nano Lett. 2 (2002) 817–822.
[4] Q. Li, S. Zhang, L. Dai, L-s. Li, Nitrogen-Doped Colloidal Graphene Quantum Dots and their Size-Dependant Electrocatalytic Activity for the Oxygen Reduction Reaction, J. Am. Chem. 134 (2012) 18932–18935.
[5] Q. Liu, X. Lu, J. Li, X. Yao, J. Li, Direct Electrochemistry of Glucose Oxidase and Electrochemical Biosensing of Glucose on Quantum Dots/Carbon Nanotubes Electrodes, Biosensors and Bioelectronics 22 (2007) 3203–3209.
[6] M. Liu, G. Shi, L. Zhang, Y. Cheng, L. Jin, Quantum Dots Modified Electrode and its Application in Electroanalysis of Hemoglobin, Electrochem. Com. 8 (2006) 305–310.
[7] D. Beitollahi, M. Hamzavi, M. Torkzadeh-Mahani, M. Shanesaz, H. Karimi Maleh, A Novel Strategy for Simultaneous Determination of Dopamine and Uric Acid using a Carbon Pased Electrode modified with CdTe Quantum Dots, Electroanalysis 27 (2015) 524–533.
[8] T. Nyokong T, in: J.H. Zagal, F. Bedioui, J.P. Dodelet (Eds.), N_4-Macrocyclic Metal Complexes, Springer, New York, 2006, pp. 315–347.
[9] A.B.P. Lever, E.R. Milaeva, in: C.C. Leznoff, A.B.P. Lever (Eds.), G. Speier in Phthalocyanines, Properties, Applications, Vol 3, VCH, New York, 1993, pp. 1.

[10] S. Khene, T. Nyokong, Redox Activity of CdTe Quantum Dots linked to Nickel Tetraaminophthalocyanine: Effects of Adsorption versus Electrodeposition on the Catalytic Oxidation of Chlorophenols, Microchem. J. 99 (2011) 478–485.
[11] S. Khene, S. Moeno, T. Nyokong, Voltammetry and electrochemical impedance spectroscopy of gold electrodes modified with CdTe quantum dots and their conjugates with nickel tetraamino Phthalocyanine, Polyhedron 30 (2011) 2162–2170.
[12] S. Nyoni, T. Nyokong, Development of Graphene/CdSe Quantum Dots-Co Phthalocyanine Nanocomposite for Oxygen Reduction Reaction, Electroanalysis 26 (2014) 2261–2272.
[13] C. Schieber, A. Bestetti, J.P. Lim, A.D. Ryan, T.-L. Nguyen, R. Eldridge, A.R. White, P.A. Gleeson, P.S. Donnelly, S.J. Williams, P. Mulvaney, Conjugation of Transferrin to Azide-modified CdSe/ZnS Core-Shell Quantum Dots using Cyclooctyne Click Chemistry Angew, Chem. Int. Ed. 51 (2012) 10523–10527.
[14] Z.P. Demko, K.B. Sharpless, A Click Chemistry Approach to Tetrazoles by Huisgen 1 3-Dipolar Cycloaddition: Synthesis of 5-Sulfonyl Tetrazoles from Azides and Sulfonyl Cyanides, Ang. Chem. Intern. Ed. 41 (2002) 2110–2113.
[15] L.L.C. Garcia, L.C.S. Figueiredo-Filhoa, G.G. Oliveira, O. Fatibello-Filho, C.E. Banks, Square-wave Voltammetric Determination of Paraquat Using a Glassy Carbon Electrode Modified with Multiwalled Carbon Nanotubes within a Dihexadecylhydrogenphosphate (DHP) Film, Sensors and Actuators B. 181 (2013) 306–311.
[16] L.C.S. de Figueiredo-Filho, V.B. dos Santos, B.C. Janegitz, T.B. Guerreiro, O. Fatibello-Filho, R.C. Faria, L.H. Marcolino-Junior, Differential Pulse Voltammetric Analysis of Paraquat using a Bisbuth Film Electrode, Electroanalysis 22 (2010) 1260–1266.
[17] S. Nyoni, T. Nyokong, Electrocatalytic Behaviour of Cobalt Tetraamino-phthalocyanine in the presence of a Composite of Reduced Graphene Nanosheets and of Multi-walled Carbon Nanotubes, Electrochimica Acta 136 (2014) 240–249.
[18] S.R. Nxele, P. Mashazi, T. Nyokong, Electrode Modification Using Alkynyl Substituted Fe(II) Phthalocyanine via Electrografting and Click Chemistry for Electrocatalysis, Electroanalysis 27 (2015) 2468–2478.
[19] Y.-F. Liu, J.-S. Yu, In-situ Synthesis of highly Luminescent Glutathione-capped CdTe/ZnS Quantum Dots with Biocompatibility, J. Colloid Interface Sci. 351 (2010) 1–9.
[20] M. Geszke, M. Murias, L. Balan, G. Medjahdi, J. Korczynski, M. Moritz, J. Lulek, R. Schneider, Folic Acid-Conjugated Core-Shell ZnS: Mn/ZnS Quantum Dots as Targeted Probes for Two-Photon Fluorescence Imaging of Cancer Cells, Acta Biomaterialia 7 (2011) 1327–1338.
[21] L. Li, J.F. Zhao, N. Won, H. Jin, S. Kim, J.Y. Chen, Quantum Dot- Aluminium Phthalocyanine Conjugates Perform Photodynamic Reactions to Kill Cancer Cells via Fluorescence Resonance Energy Transfer, Nanoscale Res. Lett. 7 (2012) 386–394.
[22] M.J. Stillman, T. Nyokong, in: C.C. Leznoff, A.B.P. Lever (Eds.), Phthalocyanines: Properties and Applications, 1, VCH, New York, 1989.
[23] R. Jenkins, R.L. Synder, Introduction to X-ray Diffractometry, Wiley and Sons, New York, 2012.
[24] D.O. Oluwole, J. Britton, P. Mashazi, T. Nyokong, Synthesis and Photophysical Properties of Nanocomposites of Aluminium Tetrasulfonated Phthalocyanine Covalently Linked to Glutathione capped CdTe/CdSe/ZnS Quantum Dots, Synthetic Metals 205 (2015) 212–221.
[25] A. Devadoss, C.E.D. Chidsey, Azide-modified Graphitic Surfaces for Covalent Attachment of Alkyne-terminated Molecules by Click Chemistry, J. Am. Chem. Soc. 12 (2007) 5370–5371.
[26] D.C. Boyd, R.T. Haasch, D.R. Mantell, R.K. Schulze, J.F. Evans, W.L. Gladfelter, Organometallic Azides as Precursors for Aluminium Nitride Thin Films, Chem. Mater. 1 (1989) 119–124.
[27] J.P. Collman, N.K. Devaraj, T.P.A. Eberspacher, C.E.D. Chidsey, Mixed Azide-terminated Monolayers: A Platform for Modifying Electrode Surfaces, Langmuir 22 (2006) 2457–2464.
[28] S. Prakash, T.M. Long, J.C. Selby, J.S. Moore, M.A. Shannon, Click Modification of Silica Surfaces and Glass Microfluidic Channels, Anal. Chem. 79 (2007) 1661–1667.
[29] A.E. Daugaard, S. Hvilsted, T.S. Hansen, N.B. Larsen, Conductive Polymer Functionalisation by Click Chemistry, Macromoles 41 (2008) 4321–4327.
[30] R.K. Schulze, D.C. Boyd, J.F. Evans, W.L. Gladfelter, A Variable Temperature X-ray Photoelectron Spectroscopic Study of the Surface Conversion of Diethylaluminium Azide to AlN, J. Vac. Sci. Tech. A 8 (1990) 2338–2343.
[31] B.P. Lever, Derivation of Metallophthalocyanine Redox Potentials via Hammet Parameter Analysis, Inorg. Chim. Acta 203 (1993) 171–174.
[32] W.A. Nevin, W. Liu, M. Melnik, A.B.P. Lever, Spectro-electrochemistry of Cobalt and Iron Tetrasulphonated Phthalocyanines, J. *Electroanal. Chem*. 213 (1986) 217–234.
[33] Yong-Ping Dong, Ting-Ting Gao, Ying Zhou, Jun-Jie Zhu, Electrogenerated Chemiluminescence Resonance Energy Transfer between Luminol and CdSe@ZnS Quantum Dots and Its Sensing Application in the Determination of Thrombin, Anal. Chem 86 (2014) 11373–11379.
[34] M. Amelia, C. Lincheneau, S. Silvi, A. Credi, Electrochemical properties of CdSe and CdTe quantum dots, Chem. Soc. Rev. 41 (2012) 5728.
[35] R.M. Elofsen, R.L. Edsberg, Polarographic Behaviour of the Viologen Indicators, Can. J. Chem. 35 (1957) 646–650.
[36] Y.Y. Wingfield, K.A. McCormack, R. Grant, Simultaneous Determination of Paraquat and Diquat in Potatoes using High Performance Capillary Electrophoresis with Ultraviolet Detection, J. Agric. Food Chem. 41 (1993) 2315–2318.
[37] C.E. Banks, R.G. Compton, New Electrodes for Old: From Carbon Nanotubes to Edge Plane Pyrolitic Graphite, Analyst 131 (2006) 15–21.
[38] D.A. Armbruster, M.D. Tillman, L.M. Hubbs, Limit of Detection (LQD)/Limit of Quantitation (LOQ): Comparison of the Empirical and the Statistical Methods Exemplified with GC-MS Assays of Abused Drugs clin, Chem. 40 (1994) 1233–1238.
[39] I.C. Lopes, D. De Souza, S.A.S. Machado, A.A. Tanaka, Voltammetric Detection of Paraquat Pesticide on a Phthgalocyanine-based Pyrolitic Graphite Electrode, Anal Bioanal Chem. 388 (2007) 1907–1914.
[40] www.hc-sc-gc.ca/ewh-semt/altformats/hecs-secs/pdf/pubs/water-eau/paraquat/paraquat-eng.pdf.
[41] M. Coates, T. Nyokong, Electrode Modification using Iron Metallophthalocyanine through Click Chemistry and Axial Ligation with Pyridine, J. Electroanal. Chem. 687 (2012) 111–116.
[42] A. Walcrius, L. Lamberts, Square wave voltammetric determination of paraquat and diquat in aqueous solution, J. Electroanal. Chem. 406 (1996) 59–68.
[43] L. Dong-ren, L. Wang-xing, Y. Zhan-hong, Q. Shin-lin, L. Ying-tao, Electrochemical investigation on kinetics of potassium intercalating into graphite in KF melt, Trans. Nonferrous Met. Soc. China 21 (2011) 166–172.
[44] K. Tyszczuk-Rotko, I. Beczkowska, A. Nasalwiercinska, Simple, selective and sensitive voltammetric method for the determination of herbicide (paraquat) using a bare boron-doped diamond electrode, Diamond related mat. 50 (2014) 86–90.
[45] H. El Harmoudi, M. Achak, S. Lahrich, A. Farahi, L. El Gaini, M. Bakasse, M.A. El Mhammedi, Square wave voltammetric determination of diquat using natural phosphate modified platinum electrode, Arab, J. Chem. (2012).
[46] T.H. Lu, I.W. Sun, Electrocatalytic determination of paraquat using nafion film coated glassy carbon electrode, Talanta 53 (2000) 443–451.